Evaluating Classical Models of Molecular Vibrations Using Raman Spectroscopy

Samuel Vasquez

May 2022

Abstract

In an attempt to find an approximate description of molecular vibrations from classical mechanics, we analyze the vibrational modes of benzene and carbon tetrachloride (CCl4) using Raman spectroscopy. We compare the Raman spectra of benzene and fully deuterated benzene with the theoretical result of classically substituting different isotope masses in the molecule, and again find that this model disagrees with the experimentally observed shift in vibrational frequencies. We compare the Raman spectra of CCl4 with predictions of the vibrational frequencies from three classical force models - a valence force model, a group theory model, and a central force model - and find that all models disagree with the experimental results. Therefore we conclude that a classical understanding of vibration and molecular structure cannot replicate the reality of molecular vibration.

1 Introduction

Due to thermal excitations, atoms in molecules vibrate about their equilibrium position. These vibrations are best described as a superposition of normal modes, which are characterized by discrete vibrational frequencies and a discrete set of excited states. The frequencies and symmetries of these vibrations are determined by the arrangement of atoms in the molecule and by interatomic bonding strength. In turn, measuring the vibrations of a molecule allows us to learn about the molecular structure of materials. Vibration, as with anything else to do with molecules, is inherently quantum mechanical. But a classical picture of vibrations in the form of coupled harmonic oscillations exists with many analogies to the full picture. Modelling quantum mechanical structures as a set of masses on classical springs cannot possibly capture their full vibrational behavior. However, such models are tremendously easier to analyze, and more computationally efficient than even the simplest ab initio quantum calculations. It would be a great accomplishment to find that there exists a model of molecular bonding that approximates the physical molecular behavior reasonably well.

1.1 Raman Scattering

Molecular vibrations are typically understood through their interaction with electromagnetic radiation. As photons are incident on sample molecules, some number of them are absorbed and contribute to vibrational excitation of the molecule. In the event that they directly excite the molecule to a higher energy state, it is called infrared (IR) absorption. In many cases, this excitation is not to an energy eigenstate, but rather to a virtual energy state from which the molecule quickly decays. In this deexcitation it emits another photon, and this is the phenomenon of light scattering. In the rare event that the molecule returns to a final vibrational state that is higher or lower than its initial vibrational state, this is called Raman scattering, or inelastic scattering. When the scattered photon has an energy lower than the initial photon, this is considered a Stokes shift, while the scattered photon having higher energy is considered an anti-Stokes shift. The energy difference between the scattered and initial photons thereby gives a direct measure of the vibrational frequencies of the molecule.

1.2 Classical and Quantum Mechanical Descriptions of Raman Scattering

Raman scattering and molecular vibrations can be understood decently well by analogy to classical systems of masses and charges and springs. An applied electric field will induce a dipole moment in a molecule's charge distribution. At high optical frequencies, the nuclei do not respond rapidly enough to follow the field, but the electron distribution does and an oscillating dipole results. The induced dipole moment is controlled by a polarizability tensor, and in the classical theory of electromagnetism, so long as the polarizability is constant, the oscillating dipole radiates energy with no change in frequency. But when the nuclei are vibrating, the electron distribution (and hence the polarizability as well) oscillates as well, giving a more sophisticated time dependence for the oscillating dipole that radiates energy at frequencies shifted by the characteristic frequency of the bond vibration. This classical treatment of vibration and light scattering successfully recovers the idea of Raman scattering and of Stokes/anti-Stokes shifting, but this only begins to describe the true phenomenon. As previously mentioned, the real character of Raman scattering is the excitation of discrete vibrational energy states and absorption/emission of photons with unequal energies. One important subtlety provided by quantum mechanical insight is that, unlike what the classical picture suggests, the Stokes and anti-Stokes shifts are not treated equivalently. The radiated photons are subjected to thermodynamic demands, and lower energy states are far more favorable than higher energy states, so the anti-Stokes intensities are strongly suppressed. And with energy states being quantized, one finds from measuring a spectrum of shifts between incoming and scattered energies that the shifts are overwhelmingly negative and peak strongly at particular values that match the discrete frequencies of vibrational energy

levels.

1.3 The Symmetry of Vibrations

An important consideration in the theory of light scattering is the role that symmetry plays in the transitions between vibrational energy states. The symmetries of molecular vibrational state wave functions give rise to selection rules that can prevent the transition between two energy levels by driving the transition moment to zero. Molecules with appreciable symmetry can have several fundamental transitions that cannot be observed from Raman scattering (ie. the vibration modes are not Raman active). Some of these selection rules also have consequence for the components of the polarizability tensor. Totally symmetric vibrations are those which preserve the symmetry of the molecule, such as radially symmetric vibrational motion. It can be found that the polarizations of scattered light (relative to the incoming linearly polarized light) is related to combinations of the tensor components of the polarizability tensor, in such a way that totally symmetric vibrational modes are the only ones that significantly preserve the polarization of incident light. Applying a polarizer to the scattered light finds that the intensity of light with polarization perpendicular to the original polarization is dramatically suppressed for frequencies that correspond to totally symmetric normal modes.

1.4 Classical Force Models

For a general model of coupled harmonic oscillators, the number of fundamental frequencies (eigenmodes) is not necessarily fewer than the number of force constants, and so the force constants are often underdetermined. One great simplification of the problem is to consider highly symmetric molecules, for which many of the force constants should be the same and the force constants are more constrained. Making more specific assumptions about the forces in the molecules also constrains the number of force constants. Therefore, we apply classical force models to experimentally observed normal modes of the tetrahedrally symmetric molecule CCl_4. The three force models are a valence force model, a "group theory" model, and a central force model.

1.4.1 CCl_4 Normal Modes

Molecules with tetrahedral symmetry have four normal modes. These are shown in figure 1.

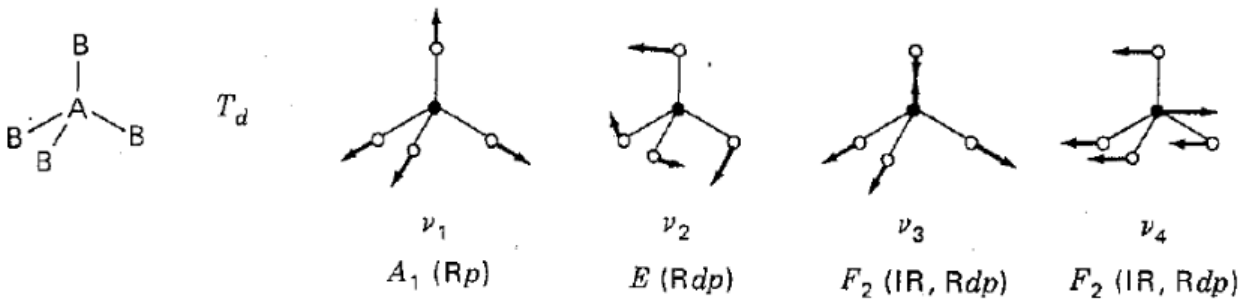

Figure 1: Vibrational eigenmodes that are found for molecules with tetrahedral symmetry. IR indicates modes that are IR active, Rp indicates Raman active modes that are polarized, and Rdp indicates depolarized Raman modes. This figure is adapted from [2].

Each eigenmode has a corresponding eigenfrequency, labelled by ν_i. Only the first eigenmode is completely symmetric, so it is polarized while the other three are unpolarized. Seeing that the ν_1 and ν_3 modes correspond to stretching motions, we can expect that these will occur at higher frequencies than the bending motions of ν_2 and ν_4.

1.4.2 Valence Force Model

First we consider a valence force model, for which we assume a Hookian spring force between the central C atom and each Cl atom in the stretching coordinates. We also assume a simple harmonic potential in the bond angles. These assumptions give a potential energy written as

$$V = \frac{1}{2}k\left(r_1^2 + r_2^2 + r_3^2 + r_4^2\right) + \frac{1}{2}k_\delta\left(\delta_{12}^2 + \delta_{13}^2 + \delta_{14}^2 + \delta_{23}^2 + \delta_{24}^2 + \delta_{34}^2\right) \tag{1}$$

where r_i is the change in the equilibrium length l of the C-Cl bonds, and δ_{ij} is the change in the angle between bonds i and j. Solving this potential for the vibrational modes gives the following relations between the vibrational eigenfrequencies and the force constants k and k_δ:

$$4\pi^2c^2\omega_1^2 = \frac{k}{m_{Cl}} \tag{2}$$

$$4\pi^2c^2\omega_2^2 = \frac{3}{m_{Cl}}\frac{k_\delta}{l^2} \tag{3}$$

$$4\pi^2c^2(\omega_3^2 + \omega_4^2) = \frac{k}{m_{Cl}}\left(1 + \frac{4m_{Cl}}{3m_C}\right) + \frac{2k_\delta}{m_{Cl}l^2}\left(1 + \frac{8m_{Cl}}{3m_C}\right) \tag{4}$$

$$16\pi^4 c^4 \omega_3^2 \omega_4^2 = \frac{2kk_\delta}{m_{Cl} l^2}\left(1 + \frac{4m_{Cl}}{m_C}\right) \tag{5}$$

m_{Cl} and m_C are the masses of chlorine and carbon respectively. $\omega_i = \nu_i/c$, with units of inverse length, are the so-called "Raman shifts" corresponding to each frequency, in the sense that the scattered photons have their energy shifted proportional to the frequency. Equations (2) and (3) determine the force constants k and k_δ. With these, (4) and (5) may be used to check the model by comparison of the observed eigenfrequencies and their values expected from this model's force constants.

1.4.3 Group Theory Model

A more complete treatment of the valence force model adds a constant k_{rr} to account for bond-bond interactions. Additional interaction terms informed by the point group corresponding to tetrahedral symmetry results in the following modified equations for the eigenfrequencies:

$$4\pi^2 c^2 \omega_1^2 = \frac{k_r + 3k_{rr}}{m_{Cl}} \tag{6}$$

$$4\pi^2 c^2 \omega_2^2 = \frac{3}{m_{Cl}} \frac{k_\delta}{l^2} \tag{7}$$

$$4\pi^2 c^2 (\omega_3^2 + \omega_4^2) = \frac{k_r - k_{rr}}{m_{Cl}}\left(1 + \frac{4m_{Cl}}{3m_C}\right) + \frac{2k_\delta}{m_{Cl} l^2}\left(1 + \frac{8m_{Cl}}{3m_C}\right) \tag{8}$$

$$16\pi^4 c^4 \omega_3^2 \omega_4^2 = \frac{2(k_r - k_{rr})k_\delta}{m_{Cl} l^2}\left(1 + \frac{4m_{Cl}}{m_C}\right) \tag{9}$$

The three force constants k_δ, k_r, and k_{rr} may be obtained from equations (6), (7), and (8). With these constants determined, we then check via (9) whether the observed eigenfrequencies agree with these force constants.

1.4.4 Central Force Model

This final model assumes that every atom exerts a Hookian force on every other atom along the lines of centers. The forces between Cl atoms have the form $F_{ClCl} = a - k_1 Q_{ij}$, where Q_{ij} is the displacement of the ith and jth Cl atoms from their equilibrium distance t. The forces between the C and each Cl atom has the form $F_{CCl} = b - k_2 r_i$, where r_i is the displacement of the C and the ith Cl atom from their equilibrium. These assumptions give a potential energy written as

$$V = -a\sum_i\sum_j Q_{ij} + \sqrt{6}a\sum_i r_i + \frac{1}{2}k_1\sum_i\sum_j Q_{ij}^2 + \frac{1}{2}k_2\sum_i r_i^2 \tag{10}$$

Solving for the vibrational eigenfrequencies gives the following:

$$4\pi^2c^2\omega_1^2 = \frac{k_2}{m_{Cl}} + 4\frac{k_1}{m_{Cl}} \tag{11}$$

$$4\pi^2c^2\omega_2^2 = \frac{k_1}{m_{Cl}} - \frac{k'}{m_{Cl}} \tag{12}$$

$$4\pi^2c^2(\omega_3^2+\omega_4^2) = \frac{2k_1}{m_{Cl}} + \frac{4m_{Cl}+3m_C}{3m_Cm_{Cl}}k_2 - \frac{2(3m_C+16m_{Cl}}{3m_Cm_{Cl}}k' \tag{13}$$

$$16\pi^4c^4\omega_3^2\omega_4^2 = \frac{2(4m_{Cl}+m_C)}{3m_Cm_{Cl}^2}(k_1k_2 - 8k_1k' - 5k_2k' - 8k'^2) \tag{14}$$

where $k' = -\frac{a}{t}$, t being the length of one edge of the tetrahedron in equilibrium position. Equations (11), (12), and (13) determine the three force constants k_1, k_2, and k'. With these, (14) serves as a check for this model.

1.5 Isotope Substitution Effect

One more assumption that can be made from classical reasoning is that when an atom of a molecule is replaced by another, the potential energy function and molecular configuration is unchanged. However, the vibrational frequencies expose this alteration because of the change in mass. This should be especially prominent in a substitution of hydrogen with deuterium, because of the very large percentage change in mass. Protons and neutrons being nearly equal in mass, the addition of one neutron to a hydrogen atom very nearly doubles its mass, while still being believable that this substitution should preserve most molecular properties. Therefore, we test the effect of isotopic substitution by measuring the fundamental frequencies of benzene and deuterated benzene, $C6H6$ and $C6D6$.

If it is indeed only the masses that change under this substitution, then the vibration frequencies of each molecule can be related by the following rule for systems of coupled oscillators:

$$\prod_{k=1}^{3N-6}\frac{\omega_k'}{\omega_k} = \prod_{i=1}^{3N}\left(\frac{m_i}{m_i'}\right)^{1/2}\left(\frac{M'}{M}\right)^{3/2}\left(\frac{I_x'I_y'I_z'}{I_xI_yI_z}\right)^{1/2} \tag{15}$$

where the primes indicate the substituted molecule, N is the number of atoms in the molecule, m_i are the atomic weights, M are the total masses of the molecules, and I are the moments of inertia.

Benzene has two completely symmetric vibration modes, which are shown in figure 2. Both modes belong to the same symmetry group. In one, the C-H bonds all stretch while the carbon ring contracts, whereas in the other, the C=C bonds all stretch while the carbon ring expands radially outward.

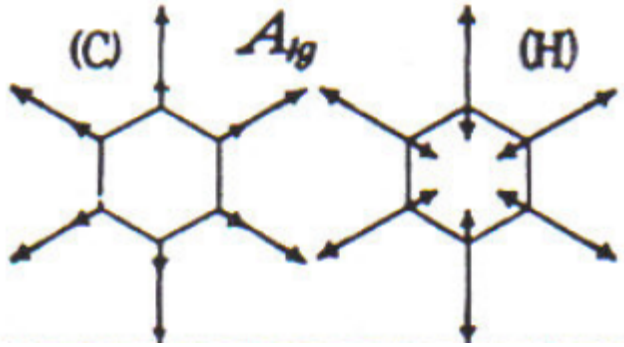

Figure 2: The two completely symmetric vibration modes of the benzene molecule. This figure is adapted from [1]

.

For these two vibration modes, formula (15) simplifies considerably to

$$\frac{\omega_1'\omega_2'}{\omega_1\omega_2} = \left(\frac{m_H}{m_D}\right)^{1/2} \approx \left(\frac{1}{2}\right)^{1/2} \approx 0.7071 \tag{16}$$

Finding the real observed eigenfrequencies of C6H6 and C6D6 and taking their product in the leftmost side of equation 16 therefore gives a simple test of whether this isotopic substitution model closely approximates molecular physics.

Section 2 will describe our apparatus and procedures for studying the vibrational frequencies of benzene and CCl4, in two parts; Section 2.1 will describe the apparatus, section 2.2 will describe the procedures for analyzing data from this equipment. Section 3 will present our results on comparing Raman spectra with our classical models. Section 3.1 will investigate the effects of substituting isotopes of different mass into the benzene molecule, sections 3.2 and 3.3 will evaluate our classical force models against CCl4 frequency data. Section 4 will conclude by reporting the results of our force model comparisons, choosing one to be the most successful, and deciding whether classical physics is an appropriate way to investigate the vibrational behavior of molecules.

2 Procedures

2.1 Apparatus

We use a BaySpec Raman spectrometer for our Raman spectrum measurements. A schematic of the spectrometer is shown in figure 3. The light source is a 532 nm laser, linearly polarized with polarization ratio of 100:1. The light is filtered through a narrow band-pass filter (F1 in the figure) to keep the light monochromatic, and it is focused into the sample vial (S). Light scattered by the sample then enters a polarization analyzer (P). The polarization analyzer allows free adjustment of its orientation to any angle relative to the incident polarization, so the spectrum can be measured for different polarization angles. Finally the light is focused on a fiber-optic coupler (FC), which transmits the scattered light into the spectrometer. The light is split into a spectrum by a transmission diffraction grating (G), and then falls across a CCD linear array of sensors which detect the intensities of each wavelength range of light and records a count of received photons into the computer software. All throughout the process, carefully-designed lenses (L1-5) and broad-band filters (F2-3) are placed to keep elastically scattered light away from the detector, as it is intense enough to overload the sensors.

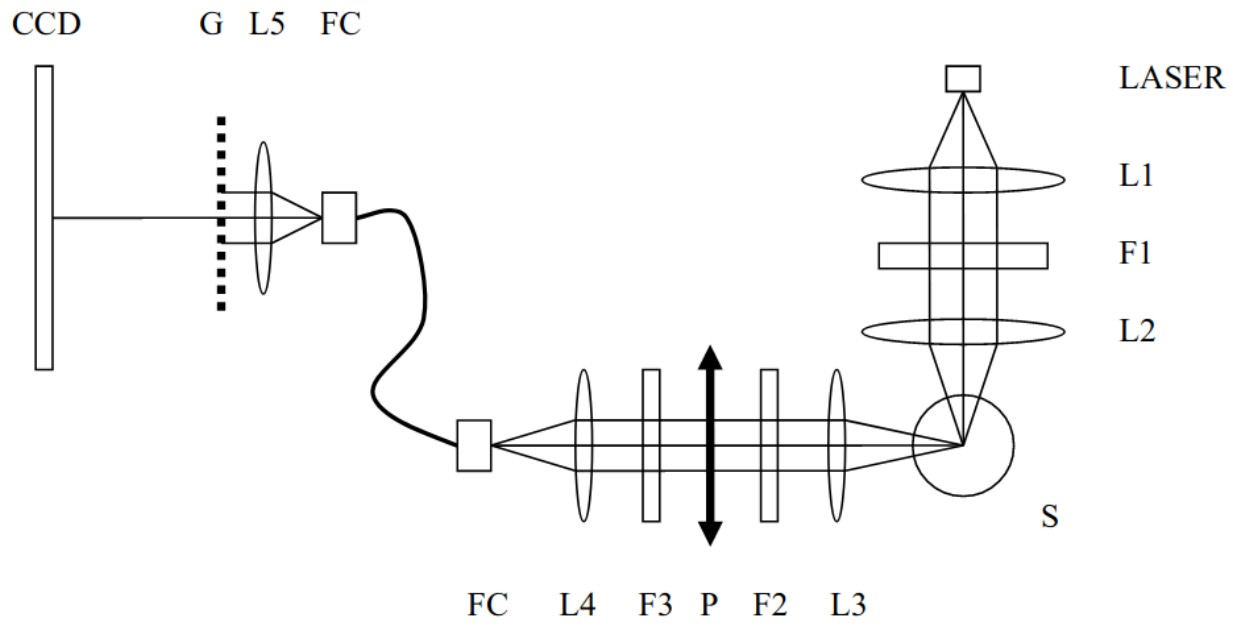

Figure 3: Schematic of the BaySpec Raman spectrometer. Source: [1]

2.2 Analysis Procedures

The computer records all data as a histogram of photon intensity for each bin of Raman shift, in units of inverse centimeters.

The Raman spectrum should have strong peaks at Raman shifts that correspond to differences in vibrational state frequencies. In order to precisely measure the locations of these peaks, we employ a simple parabolic interpolation scheme to find the maximum of each peak. Taking the center of each Raman shift bin and its intensity value as (ω_i, I_i), we take the maximum of each peak as (ω_2, I_2) and its two immediate neighbors as (ω_1, I_1) and (ω_3, I_3). Then we use these points to determine a parabola going through all three points, the maximum of which is

$$\omega_{max} = \omega_3 - \Delta\omega \left[\frac{I_3^2 - I_2^2}{I_1^2 - 2I_2^2 + I_3^2} + \frac{1}{2} \right] \tag{17}$$

where $\Delta\omega = \omega_3 - \omega_2$.

To determine an uncertainty value on these values of Raman shift, we took the spectrum of C6H6 ten times, took statistics on the three intensity values at the largest peak, and used these with equation 17 to get uncertainty in the Raman shift maximum. For simplicity, we assume that this value can be used for every frequency measurement for every peak using this algorithm, which is a fair assumption considering that every peak we measure is relatively strong and sharp. With these uncertainty values, our procedure for determining agreement between the observed fundamental frequencies and the force constant relations predicted by the classical force models will be to independently calculate left and right sides of each equation, propagate uncertainties from frequencies and atomic masses, and evaluate the difference between the left and right side calculations by the number of standard deviations separating the two values.

3 Results

Finishing with four measurements of benzene spectra and two measurements of CCl4 spectra, we were able to investigate our four classical models and their predictions, the isotope substitution model, the valence force model, the group theory model, and the central force model.

3.1 Benzene Mass Shifts

In order to determine whether it truly is the case that the substitution of one molecular atom for an isotope of different mass only has consequence on vibration frequencies and not on structure or force constants, we compared the Raman spectra of C6H6 and C6D6. The spectra are shown in figure 4, with each one showing

two spectra for two different settings of the polarization analyzer at 0 and 90 degrees polarization. The spectra for 0 degree polarization are then shown overlaid in figure 5, to show the shifts in peaks between C6H6 and C6D6.

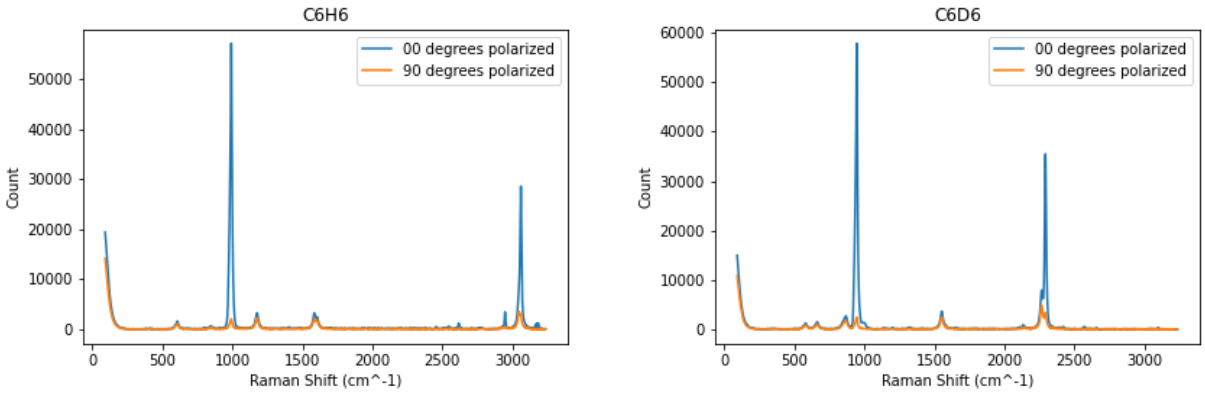

Figure 4: Observed Raman spectra of C6H6 (Left) and C6D6 (Right). Each one shows the intensities of scattered light at 0 and 90 degrees polarized relative to the incident light.

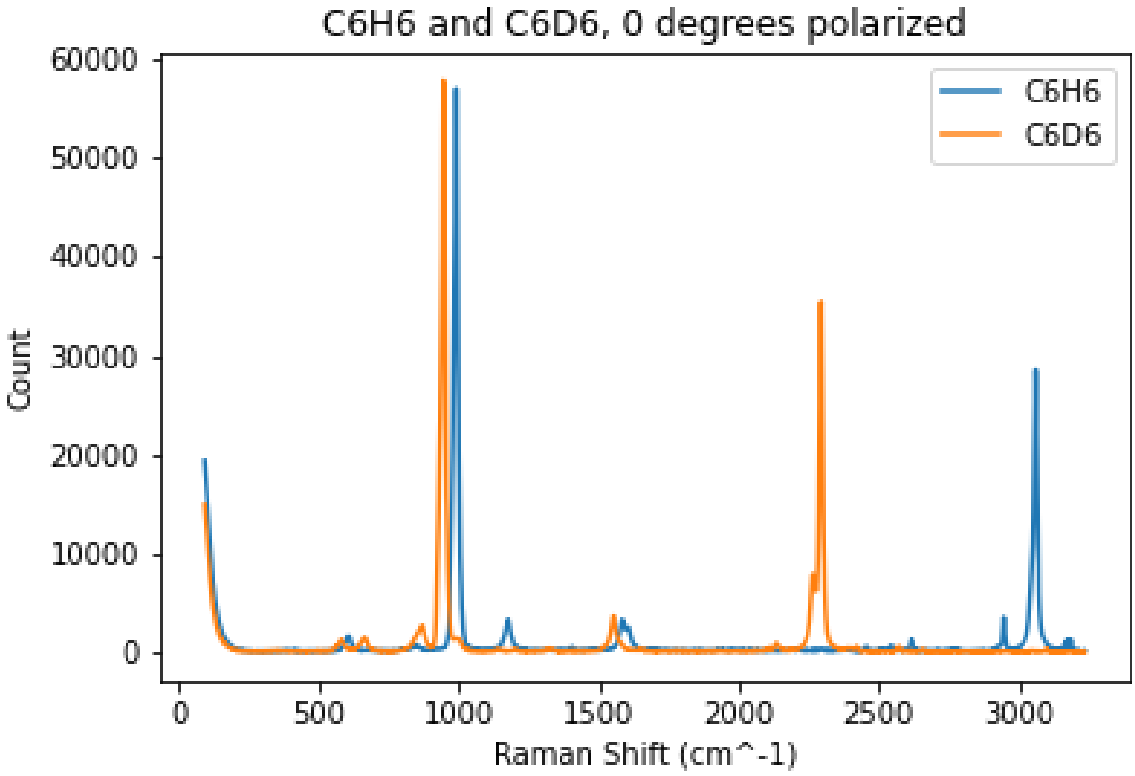

Figure 5: Benzene shifts

Looking at figure 4, by observation of the attenuation in scattered light intensity with polarization

perpendicular to incident, we find that the first and second largest peaks in both C6H6 and C6D6 are polarized, and therefore these are the two completely symmetric vibrational states from figure 2 described in section 1.4. Table 1 lists the precision measurements of each peak corresponding to the two completely symmetric vibrational modes of C6H6 and C6D6.

Table 1: Measurements of the eigenfrequencies for C6H6 and C6D6. ω_1 and ω_2 refer to the completely symmetric vibrational modes of C6H6, while ω_1' and ω_2' refer to those of C6D6.

Vibrational Mode	Raman Shift (cm^{-1})
ω_1	992.00 ± 0.95
ω_2	3061.57 ± 0.95
ω_1'	944.87 ± 0.95
ω_2'	2294.23 ± 0.95

Using these values, we evaluate equation 16 to determine its consistency with the classical prediction of isotope substitution. The ratio of frequency products is found to be

$$\frac{\omega_1'\omega_2'}{\omega_1\omega_2} = 0.7138 \pm 0.001057 \tag{18}$$

This value differs from the predicted $\frac{1}{\sqrt{2}}$ by 6.3σ, and therefore this classical isotope shift model fails to acceptably explain our observations.

3.2 Identifying CCl4 Bands

Now, turning our attention to the analysis of CCl4 and its consistency with the three classical force models, we must identify the four normal modes. Figure 6 shows our measured CCl4 spectrum, with spectra for 0 degree and 90 degree polarization.

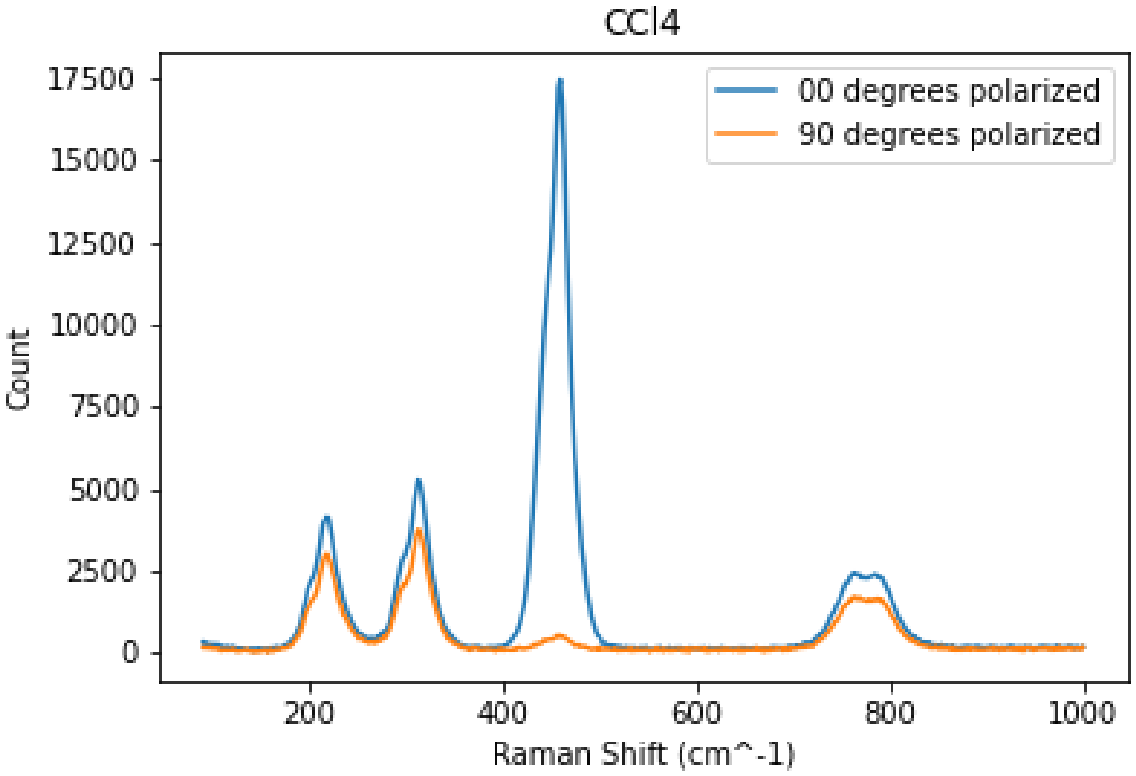

Figure 6: Observed Raman spectra of CCl4. Intensities of scattered light at 0 and 90 degrees polarized relative to the incident light are shown.

It is immediately seen that the only peak with intensity significantly attenuated under perpendicular polarization is the peak near 450 cm^{-1}, making this the completely symmetric ω_1 mode. Recalling that the ω_1 and ω_3 modes correspond to higher energy stretching motions, we can identify the peak near 800 cm^{-1} as ω_3. As for the remaining two modes, out of these two only ω_4 is IR active, and it is known from previous studies of IR spectroscopy that the only infrared band observed below 600 cm^{-1} is a feature near 300 cm^{-1}. Therefore we get that the two leftmost peaks are the ω_2 and ω_4 modes.

Before finding the precise Raman shift of each mode, it should be noted that ω_3 is exhibiting Fermi resonance. This mode is indeed a vibrational eigenmode, but it also happens to have nearly the same energy as the combination $\omega_1 + \omega_3$. This coincidence of the eigenmode and linear combination of eigenmodes having the same symmetry and nearly the same energy results in splitting, seen through the double peak. The ω_3 frequency can be taken as the mean of the doublet peaks.

With all four vibrational modes identified, their measured Raman shifts are shown in table 2.

Table 2: Measurements of the eigenfrequencies for CCl4.

Vibrational Mode	Raman Shift (cm^{-1})
ω_1	458.83 ± 0.95
ω_2	218.36 ± 0.95
ω_3	773.51 ± 0.67
ω_4	313.28 ± 0.95

3.3 Force Models

With the four fundamental frequencies measured, we now begin evaluating their agreement with the three classical force models.

3.3.1 Valence Force Model

Using equations (2) and (3) to determine the force constants k and k_δ, we find that the left and right sides of (4) are calculated to differ by 39 σ. The left and right sides of (5) differ by 32 σ. Both tests of the valence force model find very large disagreement with our observations.

3.3.2 Group Theory Model

Using equations (6), (7), and (8) to determine the force constants k_r, k_{rr}, and k_δ, we calculate that the left and right sides of (9) differ by 64 σ. This test of the group theory correction to the valence force model finds even larger disagreement with our observations.

3.3.3 Central Force Model

Using equations (11), (12), and (13) to determine the force constants k_1, k_2, and k', we calculate that the left and right sides of (14) differ by 10 σ. This test of the central force model yields the smallest disagreement of these three force models, yet still does not acceptably agree with our observations.

4 Conclusions

All of our classical models of vibrations have failed to demonstrate consistency with our experimentally measured vibrational frequencies of benzene and CCl4 via Raman spectroscopy. Our valence force model disagreed with measurements by 39σ and 32σ in two tests, our group theory model disagreed with measurements by 64σ, and our central force model disagreed with measurements by 10 σ. Of these, the most

accurate model was the central force model, but even that falls far from fitting our experimental data, and ultimately we are forced to conclude that molecules are inherently quantum mechanical and classical physics cannot appropriately describe their behavior.

References

[1] S. Garoff, B. Luokkala, and R. Schumacher. *Characterizing Molecular Vibrations Using Raman Spectroscopy*. 2017.

[2] D. P. Shoemaker et al. *Experiments in Physical Chemistry*. 4th ed. McGraw Hill, 1981, pp. 427–439.